ACS APPLIED MATERIALS & INTERFACES

Research Article

www.acsami.org

Regulated Dielectric Loss of Polymer Composites from Coating Carbon Nanotubes with a Cross-Linked Silsesquioxane Shell through Free-Radical Polymerization

Da Sun,[†] Zheng Zhou,[‡] Guang-Xin Chen,*[,†,‡] and Qifang Li*[,‡]

[†]Key Laboratory of Carbon Fiber and Functional Polymers, Ministry of Education and [‡]College of Material Science and Engineering, Beijing University of Chemical Technology, Beijing 100029, People's Republic of China

Supporting Information

ABSTRACT: We report a synthetic strategy for coating multiwalled carbon nanotubes (MWCNTs) with cross-linked octa-methacrylate-polyhedral oligomeric silsesquioxane (MA-POSS) by direct, in situ free-radical polymerization in a controlled manner. This strategy resulted in a core−shell structure with an MWCNT center. The shell thickness could be varied from ∼7 nm to 40 nm by choosing different initiators, solvents, and weight ratios of MWCNT and octa-MA-POSS. Coated MWCNT hybrids had controlled electrical performance depending on the coating layer thickness and were well-dispersed in the polymer matrix. POSS-coated MWCNTs were compounded with poly(vinylidene fluoride) to obtain a composite with high dielectric permittivity and low dielectric loss.

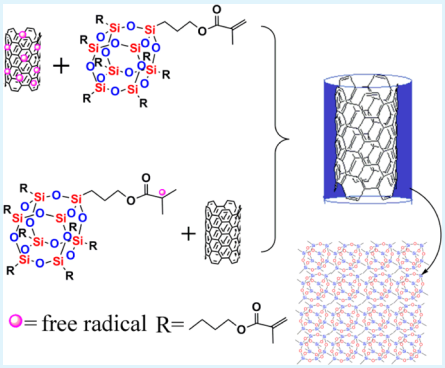

KEYWORDS: *carbon nanotubes, dielectric loss, free-radical polymerization, composites*

INTRODUCTION

Carbon nanotubes (CNTs) have attracted considerable attention since their discovery,[1] because of their unique electronic, optical, mechanical, thermal, and structural properties.[2−4] However, the strong interactions between CNTs limit their use. Researchers have proposed several methods to overcome this problem, including chemical modification,[5−7] physical absorption,[8] Friedel−Craft acylation prereaction,[9] and wrapping with polymers.[10−13] Unfortunately, these methods cannot achieve the desired results with a simple process. One of the main methods used to functionalize CNTs is to introduce carboxylic acid groups to the CNT surface by oxidation with concentrated HNO_3 and H_2SO_4 and subsequent conversion of these acids into other functional groups.[14−17] Although this method is popular and efficient, it has several disadvantages,[18] including pollution, low yield, and the additional reactions that are required. While ozone technology may introduce some functional groups to CNTs, exfoliation of CNT bundles or networks is difficult, because of the gas-phase reaction.[19] Radical polymerization is a common method in chemistry,[20] because it requires a simple process and is applicable to a wide array of monomers. Thus, many researchers have used free-radical initiators to modify the CNT surface.

Functionalizing CNTs with free radicals has been studied extensively. Ying et al.[21] first reported using benzoyl peroxide (BPO) to functionalize single-walled CNTs. Free radicals generated by decomposing BPO with alkyl iodides were used to derivatize small-diameter, single-walled CNTs. The degree of functionalization, which was estimated by thermogravimetric analysis (TGA), was as high as one in five C atoms in the nanotube framework, and the derivatized CNTs had improved solubility in organic solvents. Peng et al.[22] reported that CNTs and their fluorinated derivatives react with organic peroxides such as BPO and lauroyl peroxide to produce phenyl and undecyl sidewall-functionalized CNTs, respectively. Several researchers have used peroxy[23−27] and azo derivatives[28−31] to modify CNTs. Modified CNTs have been further processed with satisfactory results.[32,33] However, these previous studies mainly focused on grafting CNTs with small molecules or linear or branched macromolecules. In our previous work, we reported a strategy to coat CNTs with cross-linkable material by combining Diels−Alder cyclo-additions with atom transfer radical polymerization (ATRP).[34] Here, we introduce a direct radical reaction to obtain controllable surface thickness on electrically conductive CNTs. This reaction is convenient, energy-efficient, and has great industrial potential.

Polyhedral oligomeric silsesquioxane (POSS) is an organic−inorganic hybrid nanoparticle with a high melting point, low volatility, and good stability at 300 °C.[35,36] POSS also has a low dielectric constant and can improve the polymeric breakdown voltage.[37,38] Given its excellent properties and chemical structure, POSS is a good interface layer and insulative filler material. The electrical properties of the conductive filler can be controlled by adjusting the insulating interface layer, such as by

Received: June 10, 2014
Accepted: October 22, 2014
Published: October 22, 2014

applying a polymer/CNT composite dielectric material.[39] Introducing an insulating barrier layer between conductive CNTs and the polymer matrix prevents percolation after conductive particles make direct contact in the composite dielectric. Consequently, the dielectric constant improved and percolation within the material of the compound leakage current decreases. The dielectric constant of the composite material is stable with various filler contents and improves the breakdown voltage of the composite material.

In the present study, we report a synthetic strategy to coat multiwalled carbon nanotubes (MWCNTs; POS@CNTs) with cross-linked octa-methacrylate-polyhedral oligomeric silsesquioxane (MA-POSS) efficiently using direct in situ free-radical polymerization in a homogeneous system. Two typical radical initiators were used: BPO and an $FeSO_4/K_2S_2O_8$ compound. Unlike conventional functional techniques, our chemical method does not require any acid treatment of CNTs. The POS@CNTs had excellent dispersion and controlled electrical properties, thereby expanding the possible applications of polymeric composites.

EXPERIMENTAL SECTION

Materials. Multiwalled CNTs (MWCNTs, 30−45 nm in diameter and 5−15 um long, purity >98%) were purchased from Chinese Academy of Sciences Chengdu Organic Chemicals Co., Ltd. Octa-methacrylate POSS (MA-POSS) ($(C_7H_{11}O_2)_n(SiO_{1.5})_n$, where $n = 8$) was purchased from Hybrid Plastics America, as shown in Figure 1.

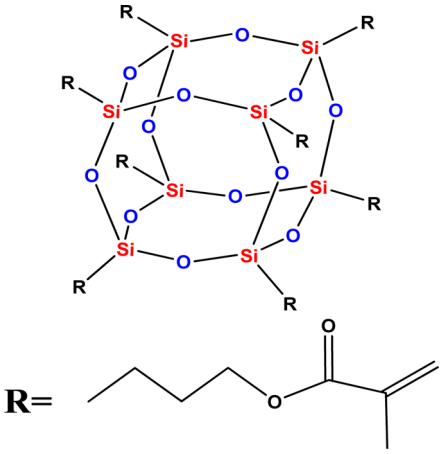

Figure 1. Molecular structure of MA-POSS.

BPO was purchased from Beijing Chemical Reagent Co., Ltd. and recrystallized with chloroform. $FeSO_4$ and $K_2S_2O_8$ were purchased from Beijing Chemical Reagent Co., Ltd. and recrystallized with deionized water. Ethanol, dimethyl sulfoxide (DMSO), dimethylformamide (DMF), acetone, and chloroform, all >99.5% purity, were purchased from Beijing Chemical Factory and used as received. Poly(vinylidene fluoride) (PVDF) was purchased from Alfa Aesar (CAS No. 24937-79-9).

Synthesis of POS@CNTs. In a typical experiment, MA-POSS (250 mg) was dissolved in 100 mL of solvent (when the radical initiator was BPO, the solvent was DMF; when the radical initiator was $FeSO_4/K_2S_2O_8$, the solvent was DMSO). The solution was poured into a three-necked round-bottom reaction flask with 50 mg of MWCNTs. After ultrasonic dispersion in an ultrasonic bath at 700 W and room temperature for 30 min, the initiator was added, the composition of which is shown in Table 1. The temperature was kept at 80 °C for BPO and 60 °C for $FeSO_4/K_2S_2O_8$ for 6 h under a nitrogen atmosphere. The mixture was then cooled to room temperature; filtered through a 0.22-μm polytetrafluoroethylene (PTFE) membrane; and washed with dimethylformamide (DMF), dimethylsulfoxide (DMSO), H_2O, C_2H_5OH, and $CHCl_3$ to remove impurities. The purified product was dried to a black powder in a vacuum oven at 45 °C overnight. The samples were named as shown in Table 1.

Table 1. Composition of Reaction Mixtures

sample	MWCNT (mg)	MA-POSS (mg)	MWCNT/MA-POSS	BPO (mg)	$FeSO_4/K_2S_2O_8$ (mg/mg)
POS@CNT-B5	50	250	1:5	12.5	0
POS@CNT-B10	50	500	1:10	25	0
POS@CNT-B15	50	750	1:15	37.5	0
POS@CNT-B20	50	1000	1:20	50	0
POS@CNT-Fe2	50	100	1:2	0	10/15
POS@CNT-Fe5	50	250	1:5	0	25/37.5
POS@CNT-Fe10	50	500	1:10	0	50/75
POS@CNT-Fe15	50	750	1:15	0	75/112.5
POS@CNT-Fe20	50	1000	1:20	0	100/150

Preparation of POS@CNT/PVDF Composites. Different amounts of POS@CNTs were blended with PVDF (1 g) in DMAc. Both POS@CNTs and PVDF were mixed with 40 mL of DMAc, separately packed in a 100-mL flask, covered with parafilm, and stirred at room temperature for 4 h. A solution containing POS@CNTs was added to the PVDF solution and stirred for another 4 h. The final mixture was dried in a vacuum oven at 70 °C overnight night to remove the solvent. Pure MWCNT/PVDF was used as a reference sample.

Characterization. Fourier transform infrared (FT-IR) spectra (Bruker Tensor 27) were used to characterize the functional groups on the CNT surface. The samples were embedded in KBr disks. X-ray photoelectron spectroscopy (XPS) was recorded on an ESCALAB 250 spectrometer (Thermo Electron Corp.) in fixed analyzer transmission mode with the Mg Kα X-ray source and a magnetic lens system that yielded high spatial resolution and high sensitivity. The pressure in the analysis chamber was 2×10^{-10} mbar. Raman spectroscopy (inVia model, Renishaw plc) at 514 nm with a 1.5 cm^{-1} resolution was used to confirm the POS@CNT structure. Thermogravimetric analysis (TGA) was conducted using a TGA system (Netzsch, Model TG209F3) in a nitrogen atmosphere. Samples were heated at a rate of 10 °C/min from 50 °C to 600 °C to determine weight loss. The morphologies of the coated MWCNTs were identified by transmission electron microscopy (TEM) (Tecnai, Model $G^2$20). The samples were dissolved in DMF and deposited dropwise onto a microgrid. The electrical resistivity of the POS@CNTs was tested with a four-probe tester (Model SZT-2, which was purchased from Suzhou Tong Chuang Electronics Co., Ltd.). The test samples were placed directly into the mold and pressed at room temperature with a manual bench press machine (Model FY-30) at 20 MPa for 10 min. Prototype test samples 10 mm in diameter and ∼1 mm thick were obtained. Dielectric constant and dielectric loss (loss tangent, tan δ) were measured (Agilent, Model 4294A with a Model 16451B fixture (40 Hz−110 MHz) at a temperature of 25 °C. Samples were prepared using a flat die rheometer (Model BL-6170C, Dongguan Bao Lun Precision Testing Instrument Co., Ltd., 4 HP) to ∼1 mm thick, and three different areas were measured from 100 MHz to 30 MHz.

RESULTS AND DISCUSSION

POS@CNTs. The POS@CNT hybrids prepared by direct free-radical polymerization were characterized by Fourier transform infrared (FT-IR) spectroscopy, which can be used to analyze the functional groups attached to the sidewalls of MWCNTs (see Figure 2). When the initiator was BPO (Figure 2A), a peak indicating Si−O−Si stretching appeared at 1120 cm^{-1}. The strength of this peak increased as the MA-POSS ratio increased, which shows that MA-POSS is attached to the MWCNTs. The C═O vibration peak at 1730 cm^{-1} fit the MA-POSS structure, which contains eight ester groups. Peaks from 2835 cm^{-1} to 3010 cm^{-1} were characterized as C−H stretching, and their intensities increased greatly after functionalization, compared with those of pristine MWCNTs. This phenomenon may be explained by alkyl groups attached to the MWCNT surface. When the initiator was the $FeSO_4/K_2S_2O_8$ redox system, similar results were achieved (Figure 2B). With the redox system, nearly all characteristic peaks were more obvious than with the BPO system, which was attributed to the ability of the initiators and solvents to trigger functionalization. This phenomenon agrees with the TEM observations.

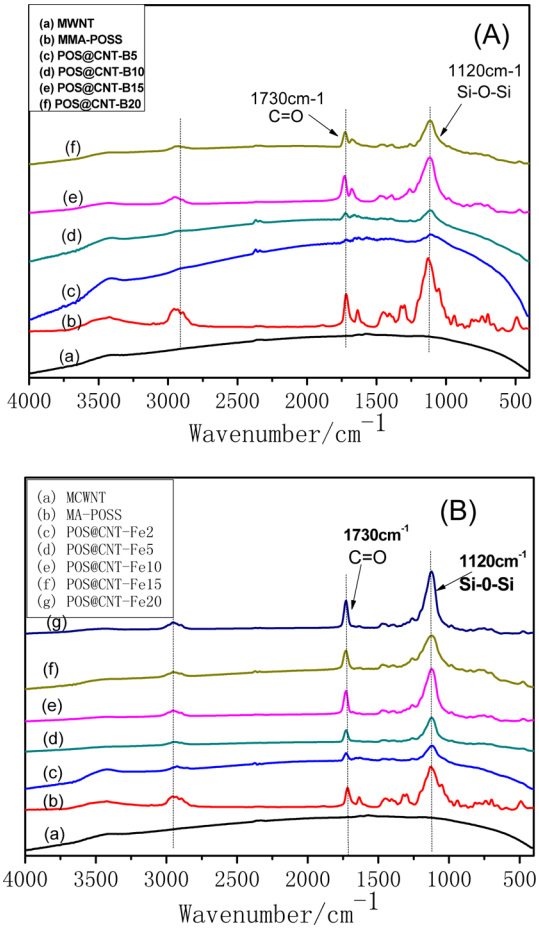

Figure 2. FT-IR spectra of POS@CNTs with (A) BPO and (B) $FeSO_4/K_2S_2O_8$ as initiators.

Attaching MA-POSS allowed us to directly observe the coated MWCNTs using TEM (Figure 3). Figure 3a shows a typical TEM image of pristine MWCNT, which has a clean and uniform surface. The image of POS@CNT-B5 in Figure 3b reveals that attaching MA-POSS produces MWCNTs with a "bumpy" sidewall ~7 nm thick. As the amount of MA-POSS increased, the core−shell structure remained the same, but the thickness of the coating layer increased to ~15 nm (Figure 3c). When the weight ratio of MA-POSS to MWCNT was <15, a thin POSS layer coated the surface of the MWCNTs. The thickness of the coating layer increased with the MA-POSS ratio. When the weight ratio of MA-POSS to MWCNT was ≥15, no separate coated MWCNTs were obtained, because the MA-POSS layers cross-linked with each other (image not shown).

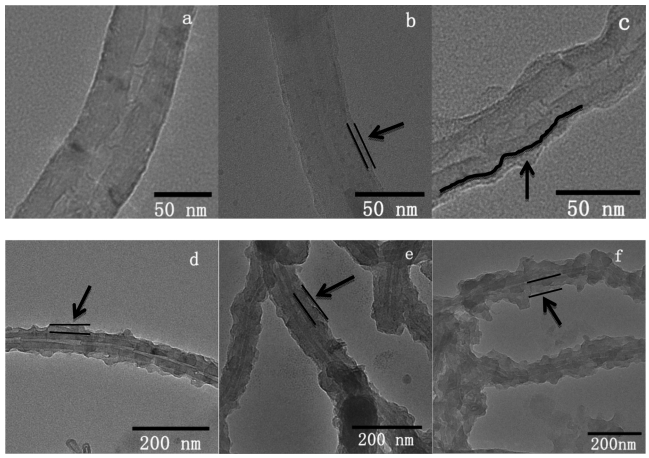

Figure 3. TEM images of (a) pristine MWCNT, (b) POS@CNT-B5, (c) POS@CNT-B10, (d) POS@CNT-Fe2, (e) POS@CNT-Fe5, and (f) POS@CNT-Fe10.

Figures 3d−f show TEM images of POS@CNTs obtained with a $FeSO_4/K_2S_2O_8$ initiator. Similar to those with the BPO system, MWCNTs had "bumpy" sidewalls, and the thickness of the shell increased with increasing MA-POSS. However, at the same weight ratio of MA-POSS to MWCNTs, the cross-linked MA-POSS layer with $FeSO_4/K_2S_2O_8$ was thicker than that with BPO. For example, as shown in Figure 3e, the POS@CNT-Fe5 layer was ~40 nm thick, which was thicker than the POS@CNT-B5 layer. At a MA-POSS to MWCNT ratio of 1:5, the coating was ~40 nm thick (Figure 3e). A core−shell hybrid of that thickness could not be obtained with BPO, because of cross-linking. As the amount of MA-POSS used increased further, the coating thickness did not increase significantly. The coating surface became rougher and MA-POSS cross-linking occurred at an MA-POSS to MWCNT ratio of 1:10 (Figure 3f). Adjusting the ratios of reactants and initiators can regulate the POSS thickness on the MWCNT surface to some extent.

To verify whether CNT surface modifications were covalent or noncovalent, Raman spectroscopy was used to characterize CNTs before and after radical functionalization (Figure 4). The change from sp^2 C to sp^3 C induced by functionalization increased the disorder band intensity. A covalent bond created between a C atom on the nanotube surface and a functional group modified the hybridization of the C atom, giving it greater sp^3 character. An increased number of surface "defects" increased the changes in the D-band intensity.[40] The Raman spectra of MA-POSS-coated MWCNTs (Figure 4) showed a large increase in the disorder-induced D-band at 1345 cm^{-1} and a broader tangential G-band at 1570 cm^{-1}, which can be attributed to covalent interactions between radicals and nanotube walls.

Considering the Raman spectra of the MWCNTs, two intense features were assigned to the D-band at 1345 cm^{-1} and

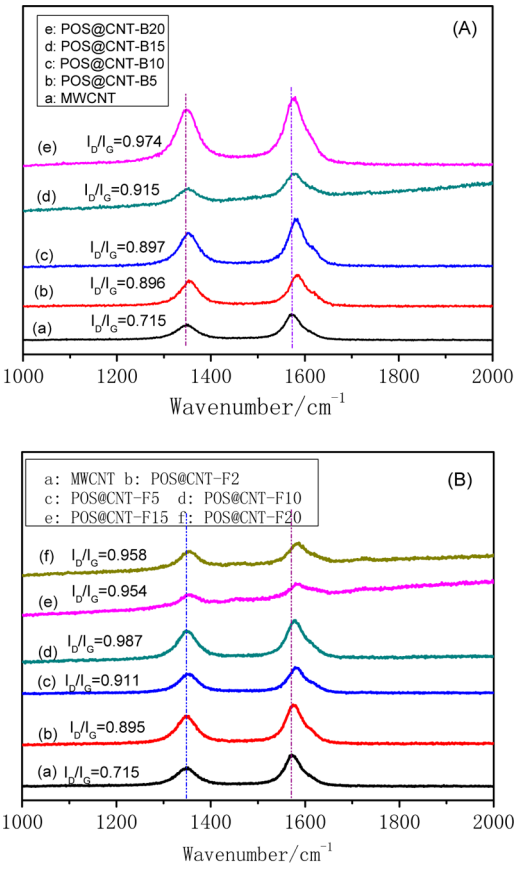

Figure 4. Raman spectra of POS@CNTs with (A) BPO and (B) $FeSO_4/K_2S_2O_8$ as initiators.

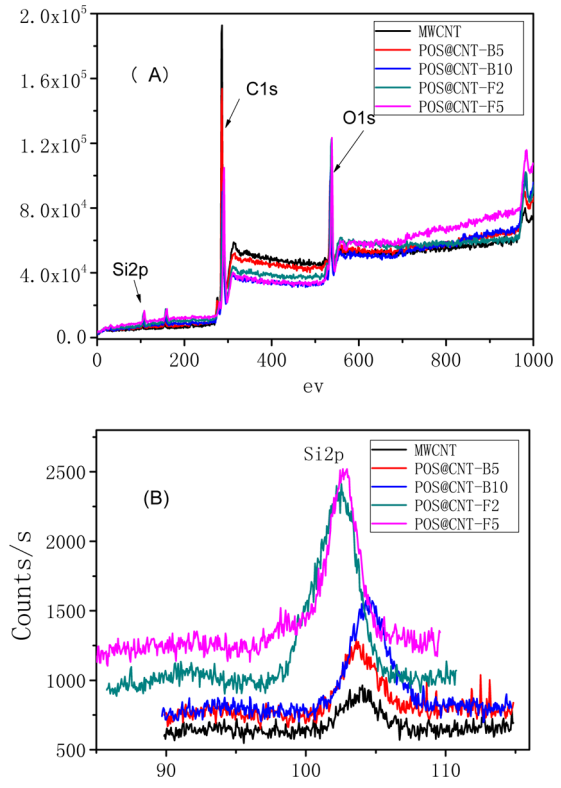

Figure 5. XPS spectra of MWCNT and POS@CNTs: (A) full scan spectra and (B) narrow scan spectra.

the G-band at 1570 cm^{-1}. The G-band was attributed to first-order scattering of the E_{2g} phonon of sp^2 C atoms, whereas the D-band was attributed to the sp^3 states of the C atom. The intensity ratios of the D- and G-bands (I_D/I_G) can be used to show disruption of the aromatic π-electrons in CNTs.[41] The I_D/I_G ratios of the hybrids in Figure 4A were 0.896 for POS@CNT-B5, 0.897 for POS@CNT-B10, 0.915 for POS@CNT-B15, and 0.974 for POS@CNT-B20, all of which were larger than that of the pristine MWCNTs (0.715). The I_D/I_G ratios of the hybrids shown in Figure 4B were 0.895 for POS@CNT-F2, 0.911 for POS@CNT-F5, 0.987 for POS@CNT-F10, 0.954 for POS@CNT-F15, and 0.958 for POS@CNT-F20, all of which were larger than that of the pristine MWCNTs (0.715).

This result indicates that numerous sp^2-hybridized C atoms were converted to sp^3-hybridized C atoms because MA-POSS was covalently attached to the MWCNT sidewalls. Using $FeSO_4/K_2S_2O_8$ as the initiator gave similar results. The results show that MA-POSS and MWCNTs were connected by covalent bonds.

Figure 5 shows the full and narrow scan Si 2p XPS spectra of five different samples. As shown in Figure 5A, the C 1s (286.9 eV), O 1s (534.81 eV), and Si 2p (104.8 eV) peaks were detected in all five samples. The oxygen concentration of MWCNTs obviously increased when coated with MA-POSS from 4.25 at. % for pristine MWCNTs to 7.57 at. % for POS@CNT-B5, 22.83 at. % for POS@CNT-B10, 22.74 at. % for POS@CNT-F2, and 20.28 at. % for POS@CNT-F5. The increased oxygen content can be attributed to the production of MWCNTs coated with MA-POSS. To further characterize the POSS coating, the Si 2p peak area of POS@CNTs was calculated and is shown in Figure 5B. The silicon concentration of MWCNTs was 2.11 at. % for pristine MWCNTs, 4.40 at. % for POS@CNT-B5, 8.99 at. % for POS@CNT-B10, 15.27 at. % for POS@CNT-F2, and 13.65 at. % for POS@CNT-F5. The fact that the silicon concentration in POS@CNTs was larger than that in pristine MWCNTs demonstrates that the MWCNTs were coated with POSSs.

TGA was used to determine the relative amounts of coating polymer on POS@CNTs (see Figure 6), because modified CNTs can be defunctionalized by thermal decomposition. The POS@CNTs coating lost considerable weight from 300 °C to 600 °C, which corresponds to decomposition of the attached MA-POSS. By contrast, the pristine MWCNTs only lost 1.3% of their weight at 600 °C in a nitrogen atmosphere. Figures 6A and 6B show that samples with different coating thicknesses lost various amounts of weight upon heating to 600 °C. The weight losses of modified MWCNTs (i.e., 11% for POS@CNT-B5, 27% for POS@CNT-B10, 38% for POS@CNT-Fe2, and 45% for POS@CNT-Fe5) were consistent with the coating thickness observed on TEM.

The results described thus far indicate that free-radical initiators can induce multifunctional monomers that contain C═C bonds to functionalize MWCNTs, leading to controllable coating of the MWCNT surface. Ying et al.[21] dispersed single-walled CNTs in benzene via ultrasonication. They found that alkyl iodides react with radicals via a diffusion-controlled process to form alkyl radicals, which then combine with the CNTs. In the present study, the initiators generated radicals through decomposition. The MA-POSS combined with these free radicals to form reactivity centers, which subsequently reacted with the MWCNTs. Zhang et al.[42] used a computer simulation to theoretically infer that the double bond on the CNT surface can be opened to participate in a polymerization

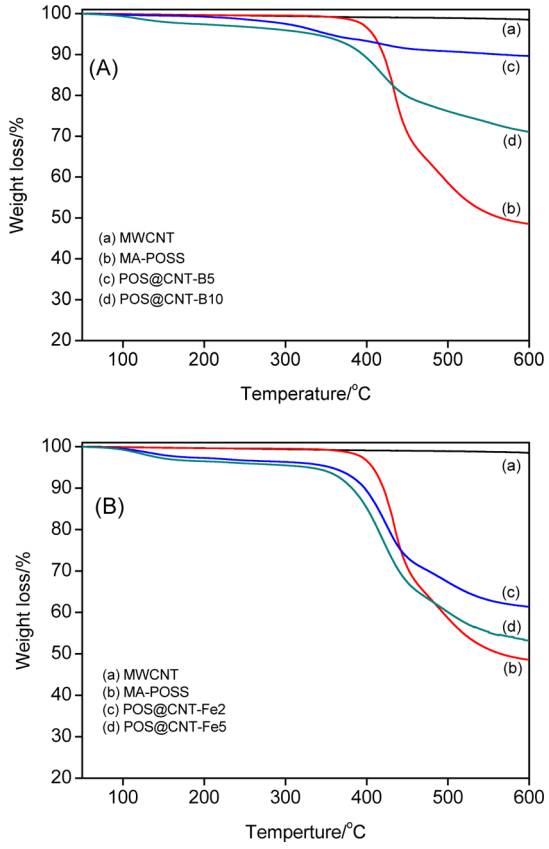

Figure 6. TGA curves of POS@CNTs with (A) BPO and (B) $FeSO_4$/$K_2S_2O_8$ as initiators.

reaction under certain conditions. They also found that suitable initiators could attack the CNTs and form CNT radicals. These new radicals are also reactive and could induce further reaction with the monomers. Our experiments support these predictions to a certain extent. We believe that the coating mechanism occurs as follows. The initiators generate radicals through decomposition. The free radicals then combine with MWCNT or MA-POSS to form a new reactivity center. Finally, the MA-POSS molecules react around the reactivity center to create an MWCNT coating.

The electrical performance of POS@CNT hybrids correlated with the thickness of the insulating POSS shell on coated MWCNTs (Table 2). The electrical resistivity of pristine

Table 2. Electrical Resistivity of Pristine MWCNT and POS@CNTs

sample	log(electrical resistivity) (Ω cm)
MWCNT	−0.125
POS@CNT-B5	0.567
POS@CNT-B10	2.541
POS@CNT-Fe2	3.399

MWCNTs (0.75 Ω cm) was smaller than that of POS@CNT hybrids (3.69 Ω cm for POS@CNT-B5, 347.6 Ω cm for POS@CNT-B10, and 2505 Ω cm for POS@CNT-Fe2). This result shows that increases in electrical resistivity were caused by larger bundles of dispersed tubes. These bundles decreased the number of tube−tube contacts, which are required for percolation. The thicker-insulating POSS layer on the surface of the MWCNT also increased the electrical resistivity. When the coating thickness exceeded 40 nm, the electrical conductivity of the hybrids decreased beyond the range of the four-probe tester used in this work.

Dielectric Properties of the POS@CNT/PVDF Composites. POS@CNT dispersion in the polymer matrix was examined via SEM. The fractured surfaces of POS@CNT-B5/PVDF composites (Figure 7) showed good dispersion of

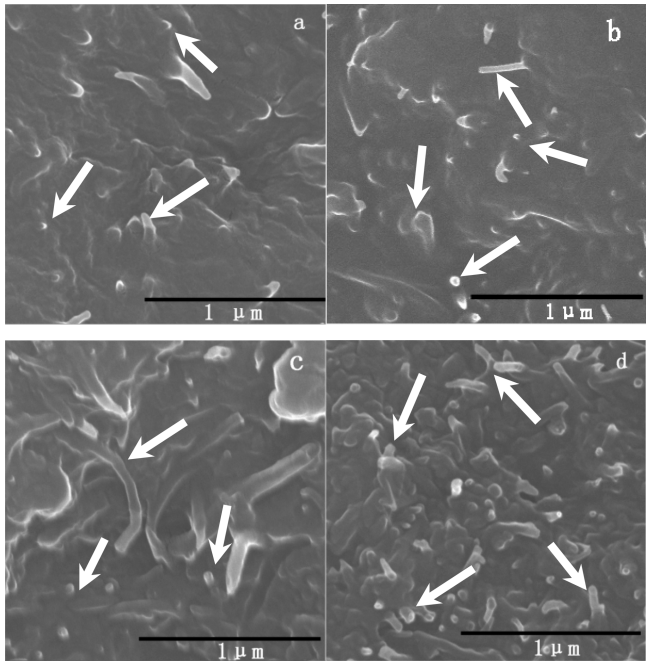

Figure 7. SEM images of POS@CNT-B5/PVDF composites with (a) 1 wt %, (b) 3 wt %, (c) 5 wt %, and (d) 7 wt % POS@CNT-B5.

MWCNTs coated with MA-POSS within the PVDF matrix. At lower filling volumes (see Figures 7a and 7b), individual MWCNTs were visible in the matrix. No agglomeration was found throughout the observation field. Even at higher filling volumes (Figures 7c and 7d), POS@CNT-B5 did not agglomerate in the matrix. A large number of nanotubes with broken ends were observed on the fracture surface, which reveals that the POSS layer improved the dispersion of coated MWCNTs within the PVDF matrix. SEM images clearly show that coated POS@CNTs were well-dispersed, rather than grafted, on the polymer matrix.

To increase the dielectric constant of a polymer by using a small amount of filler, a strategy used to fabricate percolative capacitors with conductive fillers was developed. As the volume fraction (f) of the conductive fillers approaches the vicinity of the percolation threshold (f_c), where the fillers connect with each other to form a continuous conducting path, the dielectric constant (ε) of the composites can be enhanced as described by the following power law:[43]

$$\varepsilon \propto \varepsilon_m |f - f_c|^{-s}$$

where ε_m is the dielectric constant of the matrix and s is an exponent with a value of ~1. Because of insulator−conductor transitions at the percolation threshold, the dielectric loss of percolative composites also increases in the vicinity of the percolation threshold, which counteracts the benefits of enhancing their dielectric constants.

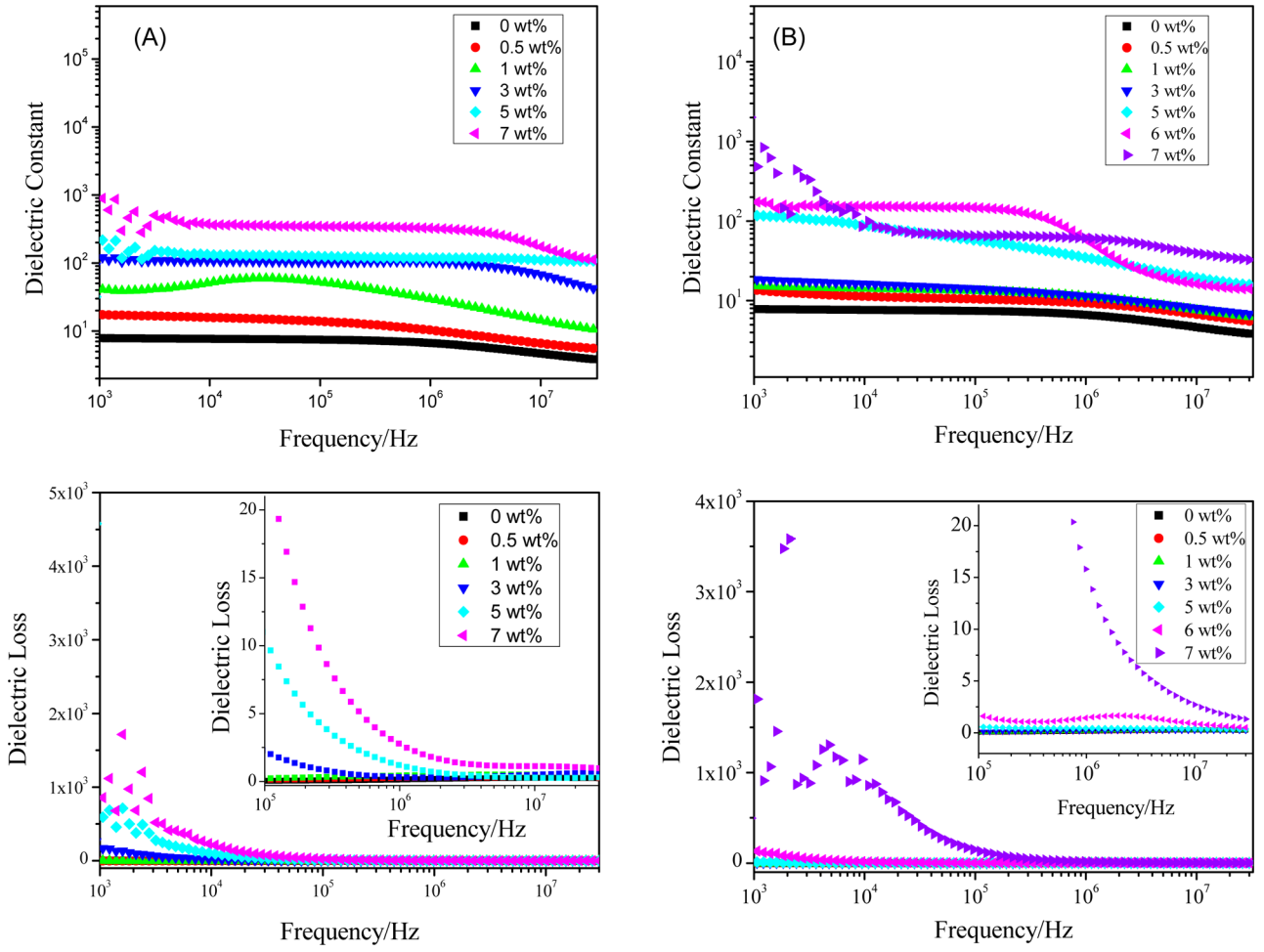

Figure 8. Dielectric constants and dielectric losses of (A) MWCNT/PVDF and (B) POS@CNT-B5/PVDF composites at different filler contents.

In this work, we used an insulated coating POSS layer to create a core−shell structured hybrid filler POS@CNT. POSS layers can reduce the dielectric loss of percolative composite capacitors by adding carbon nanotubes into polymer matrices. The dielectric loss of these percolative composites is usually high, because of insulator−conductor transitions near the percolation threshold.

The dielectric properties of the MWCNT/PVDF and POS@CNT-B5/PVDF composites are shown in Figure 8, as a function of frequency at room temperature. In all percolative polymer composites, the dielectric constant of both MWCNTs and POS@CNT-B5 increased as the filler proportions increased. CNTs formed a connection between the top and bottom electrodes, and each interparticle junction can be treated as a nanocapacitor.[44] The presence of a large number of nanocapacitors eventually forms a high dielectric composite. The pure MWCNT-based composite had a larger growth trend than the POS@CNT-B5/PVDF composite did, because the CNT surfaces of the latter were coated with a POSS layer. Although percolative polymer composites are reported to have high dielectric constants, they are not effective for embedded capacitor applications, because the conductive nature of the filler results in high dielectric loss at high filler loading levels.

As the filler proportion of MWCNTs and POS@CNT-B5 increased, the dielectric loss of the composite increased, but with different trends (see Figure 9). The dielectric loss of the pure MWCNT/PVDF composite rapidly increased with

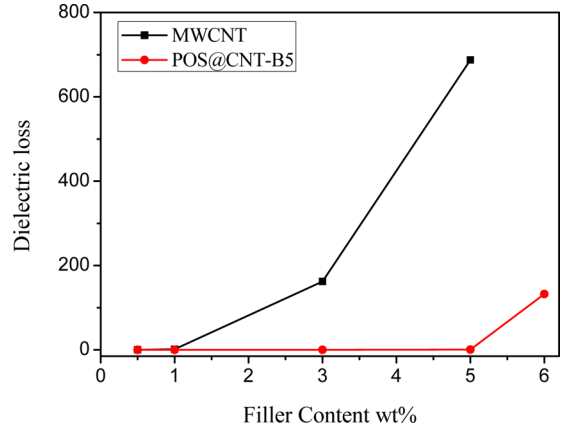

Figure 9. Dielectric loss of the POS@CNT-B5/PVDF composite at different filler contents compared with that of pure MWCNT/PVDF at 1 kHz.

increasing filler proportion; at 3 and 5 wt % MWCNTs, the dielectric losses were as high as 162.5 and 687.3, respectively, at 1 kHz. The dielectric loss of the POS@CNT-B5/PVDF composite could be controlled to levels lower than that of the pure MWCNT/PVDF composite. At 3 and 5 wt % POS@CNT-B5, the dielectric losses of the resultant composites were as low as 0.25 and 0.53, respectively, at 1 kHz. These low values

are beneficial for industrial applications of the composite materials.

The dielectric losses of the POS@CNT-B5/PVDF and MWCNTs/PVDF composites differ because of the presence of the coating layer, which serves as a barrier between CNT particles and prevents them from directly overlapping with one another. The cross-linked octa-MA-POSS has a low dielectric constant (~1.85 at 1 MHz),[37] which may also explain the relatively low dielectric loss of the POS@CNT-B5/PVDF composite. Interfaces with good integrity are desirable in reducing dielectric loss, because they provide an efficient insulating barrier to avoid quantum tunneling and suppress the resulting current leaks. The presence of a coating layer allows the dielectric loss to be controlled to low levels.

Filler/matrix interfaces play a completely different role in the electrical and dielectric constant and dielectric loss of percolative composites. Contact resistivity at the interface is less desirable for enhancing electrical conductivity, consistent with the electrical resistivity results, whereas high interfacial resistivity suppresses tunneling between adjacent fillers and leads to high-*k*, low-loss percolative composites.[39]

Unlike the dielectric of the POS@CNT-B5/PVDF composite, the dielectric constant of the POS@CNT-Fe5/PVDF composite grows slowly (Figure 10). At a filler proportion of 5 wt %, the dielectric constant of POS@CNT-Fe5/PVDF composite at 100 kHz was 12.7 (vs 57.9 for POS@CNT-B5/PVDF at the same filler proportion). Moreover, the dielectric loss of the POS@CNT-Fe5/PVDF composite at 100 kHz was only 0.065 (vs 0.55 for POS@CNT-B5/PVDF at the same filler proportion). These findings indicate that thicker POSS layers exert better barrier effects toward the CNTs than thinner POSS layers do, and thicker layers prevent direct overlaps between particles. Thus, the POS@CNT-Fe5/PVDF composite has a lower dielectric constant and dielectric loss than does the POS@CNT-B5/PVDF composite.[44]

The dielectric constant and dielectric loss for POS@CNT/PVDF composites with different filler properties are shown in Figure 11 at different frequencies. The dielectric loss of

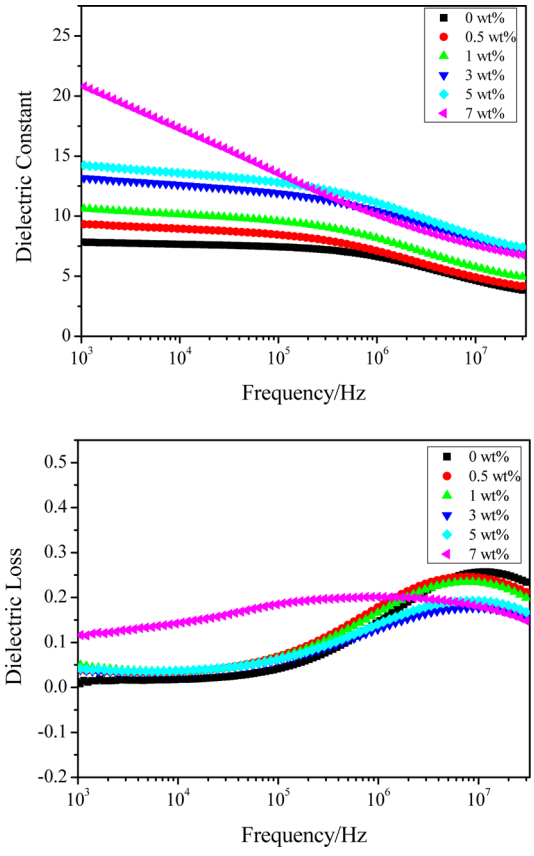

Figure 10. Variations in the dielectric constant and dielectric loss of POS@CNT-Fe5/PVDF at different filler contents.

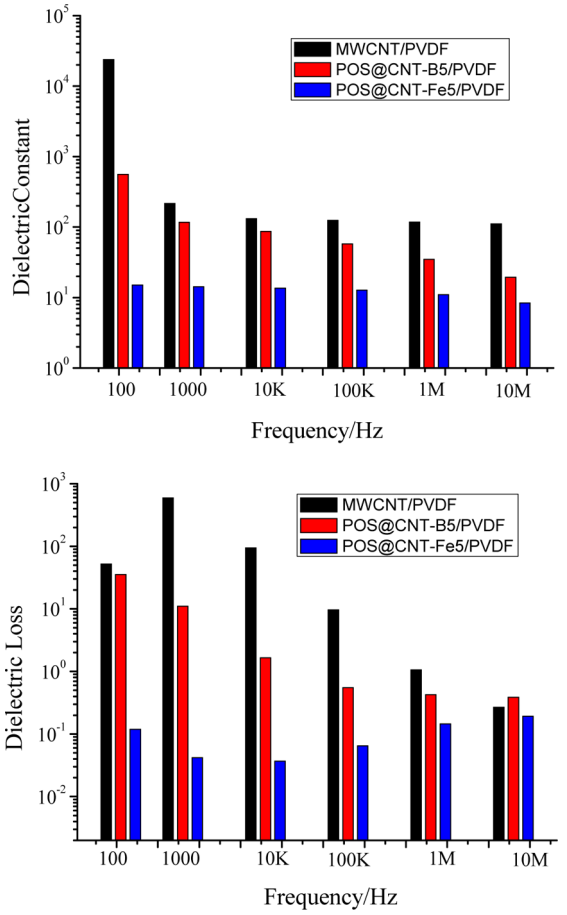

Figure 11. Relationship between the dielectric properties of POS@CNT/PVDF composites and the thickness of the POSS layer covering POS@CNTs at different frequencies and 5 wt % filler content.

MWCNT/PVDF was higher than that of POS@CNT/PVDF. This result suggests that decreases in dielectric loss were related to the thickness of the POSS layer. If the coating layer is thin, the MA-POSS coating layer may act as an interface and help MWCNTs disperse into the PVDF matrix to prevent them from overlapping. Consequently, percolation is avoided and dielectric loss is controlled within a relatively low range.

CONCLUSION

In this study, carbon nanotubes (CNTs) were successfully functionalized by a fairly simple and low-cost approach involving a one-step operation that is environmentally friendly and energy-efficient. Pristine multiwalled carbon nanotubes (MWCNTs) were successfully coated with a monomer containing multiple C═C bonds, MA-POSS, in a controlled manner by direct in situ free-radical polymerization initiated by either BPO or the $FeSO_4/K_2S_2O_8$ redox system. MA-POSS coatings of various thickness were achieved by adjusting the

ratio of reactants or selecting an appropriate reaction system. At a constant MA-POSS to MWCNT weight ratio, the thickness of the cross-linked MA-POSS on the MWCNTs ranged from ~25 nm to ~40 nm in the $FeSO_4/K_2S_2O_8$ redox system, which is higher than that achieved with BPO (~7−15 nm). The coated MWCNTs had controllable electrical performance that varied according to the thickness of the POSS layer. The coated MWCNTs were well-dispersed in a PVDF matrix, and the PVDF composites had high dielectric constants and low dielectric loss. The dielectric loss of composites was easily controlled by adjusting the thickness of the POSS layer.

■ ASSOCIATED CONTENT

Ⓢ Supporting Information

This material is available free of charge via the Internet at http://pubs.acs.org.

■ AUTHOR INFORMATION

Corresponding Authors

*Tel./Fax: +86 10 64421693. E-mail: gxchen@mail.buct.edu.cn (G. X. Chen).

*Tel./Fax: +86 10 64421693. E-mail: qflee@mail.buct.edu.cn (Q. Li).

Notes

The authors declare no competing financial interest.

■ ACKNOWLEDGMENTS

The authors gratefully acknowledge financial support for this work coming from the National Natural Science Foundation of China (NSFC) (No. 51173009).

■ REFERENCES

(1) Iijima, S. Helical Microtubules of Graphitic Carbon. *Nature* **1991**, *354*, 56−58.

(2) Ajayan, P. Nanotubes from Carbon. *Chem. Rev.* **1999**, *99*, 1787.

(3) Baughman, R. H.; Zakhidov, A. A.; de Heer, W. A. Carbon Nanotubes—The Route Toward Applications. *Science* **2002**, *297*, 787−792.

(4) Chen, G.; Kim, H.; Park, B.; Yoon, J. Multi-walled Carbon Nanotubes Reinforced Nylon 6 Composites. *Polymer* **2006**, *47*, 4760−4767.

(5) Sun, Y.-P.; Fu, K.; Lin, Y.; Huang, W. Functionalized Carbon Nanotubes: Properties and Applications. *Acc. Chem. Res.* **2002**, *35*, 1096−1104.

(6) Dyke, C. A.; Tour, J. M. Overcoming the Insolubility of Carbon Nanotubes Through High Degrees of Sidewall Functionalization. *Chem.—Eur. J.* **2004**, *10*, 812−817.

(7) Chen, G. X.; Kim, H. S.; Park, B. H.; Yoon, J. S. Highly Insulating Silicone Composites With a High Carbon Nanotube Content. *Carbon* **2006**, *44*, 3373−3375.

(8) Chen, G. X.; Li, Y. J.; Shimizu, H. Ultrahigh-shear Processing for the Preparation of Polymer/Carbon Nanotube Composites. *Carbon* **2007**, *45*, 2334−2340.

(9) Nayak, R. R.; Shanmugharaj, A. M.; Ryu, S. H. A Novel Route for Polystyrene Grafted Single-walled Carbon Nanotubes and their Characterization. *Macromol. Chem. Phys.* **2008**, *209*, 1137−1144.

(10) Rouse, J. H. Polymer-Assisted Dispersion of Single-walled Carbon Nanotubes in Alcohols and Applicability Toward Carbon Nanotube/Sol−Gel Composite Formation. *Langmuir* **2005**, *21*, 1055−1061.

(11) Dieckmann, G. R.; Dalton, A. B.; Johnson, P. A.; Razal, J.; Chen, J.; Giordano, G. M.; Muñoz, E.; Musselman, I. H.; Baughman, R. H.; Draper, R. K. Controlled Assembly of Carbon Nanotubes by Designed Amphiphilic Peptide Helices. *J. Am. Chem. Soc.* **2003**, *125*, 1770−1777.

(12) Star, A.; Steuerman, D. W.; Heath, J. R.; Stoddart, J. F. Starched Carbon Nanotubes. *Angew. Chem., Int. Ed.* **2002**, *41*, 2508−2512.

(13) Ojha, L. R.; Tchoul, M. N.; Bastola, K. P.; Ausman, K. D. Crosslinked Polymer Sheaths for Dispersing Individual Single-walled Carbon Nanotubes in Nonaqueous Solvents. *Nanotechnology* **2013**, *24*, 435602.

(14) Chen, J.; Hamon, M. A.; Hu, H.; Chen, Y.; Rao, A. M.; Eklund, P. C.; Haddon, R. C. Solution Properties of Single-walled Carbon Nanotubes. *Science* **1998**, *282*, 95−98.

(15) Chen, G.-X.; Kim, H. S.; Park, B. H.; Yoon, J. S. Controlled Functionalization of Multiwalled Carbon Nanotubes with Various Molecular-weight Poly(L-lactic acid). *J. Phys. Chem. B* **2005**, *109*, 22237−22243.

(16) Chen, G. X.; Kim, H. S.; Park, B. H.; Yoon, J. S. Synthesis of Poly(L-lactide)-functionalized Multiwalled Carbon Nanotubes by Ring-opening Polymerization. *Macromol. Chem. Phys.* **2007**, *208*, 389−398.

(17) Chen, G.-X.; Shimizu, H. Multiwalled Carbon Nanotubes Grafted with Polyhedral Oligomeric Silsesquioxane and its Dispersion in Poly(L-lactide) Matrix. *Polymer* **2008**, *49*, 943−951.

(18) Gao, C.; He, H.; Zhou, L.; Zheng, X.; Zhang, Y. Scalable Functional Group Engineering of Carbon Nanotubes by Improved One-step Nitrene Chemistry. *Chem. Mater.* **2008**, *21*, 360−370.

(19) Byl, O.; Liu, J.; Yates, J. T. Etching of Carbon Nanotubes by Ozone: A Surface Area Study. *Langmuir* **2005**, *21*, 4200−4204.

(20) Veregin, R. P. N.; Georges, M. K.; Kazmaier, P. M.; Hamer, G. K. Free Radical Polymerizations for Narrow Polydispersity Resins: Electron Spin Resonance Studies of the Kinetics and Mechanism. *Macromolecules* **1993**, *26*, 5316−5320.

(21) Ying, Y.; Saini, R. K.; Liang, F.; Sadana, A. K.; Billups, W. Functionalization of Carbon Nanotubes by Free Radicals. *Org. Lett.* **2003**, *5*, 1471−1473.

(22) Peng, H.; Reverdy, P.; Khabashesku, V. N.; Margrave, J. L. Sidewall Functionalization of Single-walled Carbon Nanotubes with Organic Peroxides. *Chem. Commun. (Cambridge, U.K.)* **2003**, 362−363.

(23) Umek, P.; Seo, J. W.; Hernadi, K.; Mrzel, A.; Pechy, P.; Mihailovic, D. D.; Forró, L. Addition of Carbon Radicals Generated from Organic Peroxides to Single Wall Carbon Nanotubes. *Chem. Mater.* **2003**, *15*, 4751−4755.

(24) Peng, H.; Alemany, L. B.; Margrave, J. L.; Khabashesku, V. N. Sidewall Carboxylic Acid Functionalization of Single-walled Carbon Nanotubes. *J. Am. Chem. Soc.* **2003**, *125*, 15174−15182.

(25) Qin, S.; Qin, D.; Ford, W. T.; Herrera, J. E.; Resasco, D. E.; Bachilo, S. M.; Weisman, R. B. Solubilization and Purification of Single-wall Carbon Nanotubes in Water by in situ Radical Polymerization of Sodium 4-Styrenesulfonate. *Macromolecules* **2004**, *37*, 3965−3967.

(26) Hu, H.; Hui, K.; Hui, K.; Lee, S.; Zhou, W. Facile and Green Method for Polystyrene Grafted Multi-Walled Carbon Nanotubes and Their Electroresponse. *Colloids Surf. A* **2012**, *396*, 177−181.

(27) Engel, P. S.; Billups, W. E.; Abmayr, D. W.; Tsvaygboym, K.; Wang, R. Reaction of Single-Walled Carbon Nanotubes with Organic Peroxides. *J. Phys. Chem. C* **2008**, *112*, 695−700.

(28) Bahr, J. L.; Yang, J.; Kosynkin, D. V.; Bronikowski, M. J.; Smalley, R. E.; Tour, J. M. Functionalization of Carbon Nanotubes by Electrochemical Reduction of Aryl Diazonium Salts: A Bucky Paper Electrode. *J. Am. Chem. Soc.* **2001**, *123*, 6536−6542.

(29) Guo, G.; Yang, D.; Wang, C.; Yang, S. Fishing" Polymer Brushes on Single-walled Carbon Nanotubes by in-situ Free Radical Polymerization in a Poor Solvent. *Macromolecules* **2006**, *39*, 9035−9040.

(30) Yang, Y.; Qiu, S.; Xie, X.; Wang, X.; Li, R. K. Y. A Facile, Green, and Tunable Method to Functionalize Carbon Nanotubes with Water-soluble Azo Initiators by One-step Free Radical Addition. *Appl. Surf. Sci.* **2010**, *256*, 3286−3292.

(31) Yuen, S.-M.; Ma, C.-C. M.; Chuang, C.-Y.; Yu, K.-C.; Wu, S.-Y.; Yang, C.-C.; Wei, M.-H. Effect of Processing Method on the Shielding Effectiveness of Electromagnetic Interference of MWCNT/PMMA Composites. *Compos. Sci. Technol.* **2008**, *68*, 963−968.

(32) Zhang, F.; Guo, G.; Fang, J. Highly Dense and Uniformly Dispersed Platinum Nanoparticles on Poly (acrylic acid) Modified Multi-walled Carbon Nanotubes for Methanol Oxidation. *Mater. Res. Bull.* **2011**, *46*, 905−909.
(33) Peng, M.; Liao, Z.; Zhu, Z.; Guo, H. A Simple Polymerizable Polysoap Greatly Enhances the Grafting Efficiency of the "Grafting-to" Functionalization of Multiwalled Carbon Nanotubes. *Macromolecules* **2010**, *43*, 9635−9644.
(34) Zhang, W.; Zhou, Z.; Li, Q.; Chen, G.-X. Controlled Dielectric Properties of Polymer Composites from Coating Multiwalled Carbon Nanotubes with Octa-acrylate Silsesquioxane through Diels−Alder Cycloaddition and Atom Transfer Radical Polymerization. *Ind. Eng. Chem. Res.* **2014**, *53*, 6699−6707.
(35) Fina, A.; Monticelli, O.; Camino, G. POSS-based Hybrids by Melt/reactive Blending. *J. Mater. Chem.* **2010**, *20*, 9297−9305.
(36) Milliman, H. W.; Ishida, H.; Schiraldi, D. A. Structure Property Relationships and the Role of Processing in the Reinforcement of Nylon 6-POSS Blends. *Macromolecules* **2012**, *45*, 4650−4657.
(37) Liu, Y. L.; Tseng, M. C.; Fangchiang, M. H. Polymerization and Nanocomposites Properties of Multifunctional Methylmethacrylate POSS. *J. Polym. Sci., Part A: Polym. Chem.* **2008**, *46*, 5157−5166.
(38) Horwath, J. C.; Schweickart, D. L.; Garcia, G.; Klosterman, D.; Galaska, M.; Schrand, A.; Walko, L. C. Improved Electrical Properties of Epoxy Resin with Nanometer-Sized Inorganic Fillers. In *Conference Record of the 2006 Twenty-Seventh International Power Modulator Symposium*; IEEE: Piscataway, NJ, 2006; pp 189−191.
(39) Nan, C. W.; Shen, Y.; Ma, J. Physical Properties of Composites Near Percolation. *Annu. Rev. Mater. Res.* **2010**, *40*, 131−151.
(40) Dresselhaus, M. S.; Dresselhaus, G.; Saito, R.; Jorio, A. Raman Spectroscopy of Carbon Nanotubes. *Phys. Rep.* **2005**, *409*, 47−99.
(41) Zhang, K.; Choi, H. J. Carboxylic Acid Functionalized MWNT Coated Poly (methyl methacrylate) Microspheres and Their Electro-response. *Diamond Relat. Mater.* **2011**, *20*, 275−278.
(42) Mylvaganam, K.; Zhang, L. Nanotube Functionalization and Polymer Grafting: An Ab Initio Study. *J. Phys. Chem. B* **2004**, *108*, 15009−15012.
(43) Nan, C.-W. Physics of Inhomogeneous Inorganic Materials. *Prog. Mater. Sci.* **1993**, *37*, 1−116.
(44) Shen, Y.; Lin, Y.; Nan, C. W. Interfacial Effect on Dielectric Properties of Polymer Nanocomposites Filled with Core/Shell-Structured Particles. *Adv. Funct. Mater.* **2007**, *17*, 2405−2410.